

# SUPERSONIC LAMINAR FLOW CONTROL INVESTIGATIONS WITHIN THE SUPERTRAC PROJECT

D. Arnal

ONERA/DMAE centre de Toulouse  
2 avenue Edouard Belin, 31055 Toulouse Cedex 4  
France

## ABSTRACT

The global objective of the SUPERTRAC project (beginning 2005-end 2007) is to explore the possibilities to delay laminar-turbulent transition on supersonic aircraft wings. Several techniques are investigated: micron-sized roughness elements, anti-contamination devices, suction and shape optimization. This paper provides an overview of the project structure and summarizes the results obtained during the first 30 months. These results mainly include fundamental experiments in the S2MA and RWG wind tunnels as well as a numerical optimization of a supersonic aircraft wing in flight conditions. As a conclusion, some hints concerning the compatibility of different control techniques are suggested.

## 1. INTRODUCTION

The European project SUPERTRAC (SUPERsonic TRAnSition Control) was started on January 1<sup>st</sup>, 2005, with the co-ordination of ONERA as a Specific Targeted Research Project (STReP) of the 6<sup>th</sup> EU framework program. The global objective of this project is to carry out fundamental, numerical and experimental investigations for evaluating the possibilities of laminar flow control on supersonic civil aircraft wings.

Laminar flow can be achieved by delaying the onset of laminar-turbulent transition on the wings using specific tools such as shape optimization, suction, micron-sized roughness elements. Reducing the extent of turbulent flow is of considerable practical interest because it reduces the friction drag. It also contributes to satisfy the severe requirements on emission and noise, because drag reduction is directly related to the reduction of weight and size, as well as fuel burn and noise. Laminar flow control techniques have been widely tested for subsonic and transonic flows, but little is known about their extension to supersonic flows. This justifies the work undertaken within SUPERTRAC.

The SUPERTRAC consortium of 9 partners includes two European airframe manufacturers (Airbus and Dassault Aviation), 4 research centres (ONERA in France, CIRA in Italy, DLR in Germany, FOI in Sweden), 2 universities (IST in Portugal, KTH in Sweden) and one SME (IBK in Germany).

SUPERTRAC has a total run time of 36 months and will end (in principle) in December 2007. The present paper gives an overview of the main achievements of the project at mid-2007. The overall structure of SUPERTRAC and the available theoretical/numerical tools for transition prediction are presented in paragraph 2. The next three paragraphs are devoted to a more detailed description of the results obtained so far. Fundamental experiments on two constant chord models are described in paragraphs 3 and 4, respectively. Paragraph 5 deals with a numerical optimization of an aircraft wing exhibiting natural laminar flow. The compatibility between the different control techniques is finally discussed.

## 2. OVERVIEW OF THE SUPERTRAC PROJECT

### 2.1. Transition mechanisms

#### 2.1.1. Natural transition

“Natural” transition is triggered by the breakdown of unstable waves generated by the disturbances present in the free-stream (noise) or at the wall (surface polishing). On a swept wing, distinction is made between Tollmien-Schlichting (TS) and crossflow (CF) waves. TS waves are the result of the instability of the streamwise mean velocity profile. They develop in regions of zero or positive pressure gradients. CF waves are the result of the instability of the crossflow mean velocity profile. They are unstable in regions of negative pressure gradient, typically in the vicinity of the leading edge of swept wings where the flow is strongly accelerated. A peculiar feature of CF instability is that zero frequency waves are highly amplified. They take the form of stationary vortices practically aligned with the external streamlines. Their initial amplitude depends on the model surface polishing.

Delaying the onset of transition requires to modify the mean velocity field and/or the instability mechanisms in such a way that the growth rate of TS and CF waves is reduced. Three strategies are currently used for this purpose: NLF (Natural Laminar Flow, i.e. optimization of the pressure distribution on the wing), LFC (Laminar Flow Control by application of a small amount of suction) and HLFC (Hybrid Laminar Flow Control) which

combines the previous two approaches.

Quite recently, an innovative solution for transition control has been proposed by W.S. Saric at Arizona State University [1,2,3]. It is based on the fact that stationary vortices dominate the transition process when CF instability plays the dominant role. These natural stationary vortices have a wavelength which can be easily computed from the linear stability theory. The idea is to artificially create other stationary vortices by using a spanwise row of micron-sized roughness elements close to the leading edge. The wavelength of the new vortices corresponds to the spacing between the roughness elements. For particular values of this wavelength and for particular pressure gradients (to be optimized), the nonlinear interactions between natural and artificial vortices result in a reduction of the amplitude of the natural vortices (target modes); at the same time, if the amplitude of the artificial vortices (killer modes) remains below some critical threshold, transition is delayed.

### 2.1.2. Leading edge contamination

The efforts to laminarise a swept wing can be annihilated by leading edge contamination. This phenomenon occurs when the turbulence convected along the fuselage (or along the wind tunnel wall) propagates along the swept leading edge and spreads over the wing surface. For low speed flows, the relevant parameter is the leading edge Reynolds number  $\bar{R}$ . For a cylinder of radius  $R$ ,  $\bar{R}$  is expressed as:

$$\bar{R} = \left[ \frac{V_0 R \sin \varphi \operatorname{tg} \varphi}{\nu} \right]^{1/2}$$

$V_0$  is the free stream velocity,  $\varphi$  is the sweep angle and  $\nu$  is the kinematic viscosity. Experiments have shown that leading edge contamination occurs as soon as  $\bar{R}$  exceeds a critical value around 250 [4,5]. For compressible flows, the same criterion can be applied by using a modified Reynolds number  $\bar{R}^*$  deduced from  $\bar{R}$  by an empirical compressibility function [6].

In many practical problems (flight conditions), the critical value of  $\bar{R}^*$  is exceeded, so that leading edge contamination is likely to occur. In order to delay the onset of this parasitic phenomenon, specific tools need to be developed. In subsonic and transonic flows, Gaster bumps and localised suction along the attachment line have proven their efficiency [7], but the state-of-the-art is very poor for supersonic flows.

### 2.2. Natural transition prediction

The linear stability theory is widely used to describe the development of unstable waves responsible for natural transition. In the framework of the so-called “local” approach, the disturbances are written as:

$$r' = \hat{r}(y) \exp[i(\alpha x + \beta z - \omega t)]$$

$r'$  is a velocity, pressure or density fluctuation.  $\hat{r}$  is an amplitude function.  $x$  and  $z$  are the directions normal and parallel to the leading edge,  $y$  is the direction normal to the wall. In the framework of the spatial theory,  $\alpha = \alpha_r + i\alpha_i$  is the (complex) wave number in the  $x$  direction.  $\beta$  and  $\omega$  are real and represent the wave number in the  $z$  direction and the frequency. Introducing the previous expression into the linearized Navier-Stokes equations and assuming that the mean flow is parallel, leads to a system of ordinary differential equations for the amplitude functions (eigenvalue problem).

The linear PSE (Parabolized Stability Equations) or “non local” approach provides an improvement to the classical theory [8]. The mean flow field and the amplitude functions now depend on both  $x$  and  $y$ , and  $\alpha$  depends on  $x$ . With the assumption that the  $x$ -dependence is slow, the numerical problem consists in solving a set of (nearly) parabolic equations in  $x$ , with initial disturbance profiles specified at some starting point  $x_0$ .

To predict transition, the most popular method is the  $e^N$  criterion, see review in [9]. The so-called  $N$  factor is the total growth rate of the most unstable disturbances. It is computed by integrating  $-\alpha_i$  in the streamwise direction. Transition is assumed to occur for some specified value  $N_t$  of  $N$ ; for instance,  $N_t$  lies in the range 8-10 on two-dimensional (2D) airfoils in low turbulence wind tunnels.

The main interest of the linear PSE is to provide initial conditions for the nonlinear PSE which simulate the nonlinear wave interactions [8]. The disturbances are now expressed as a double series of  $(n, m)$  modes of the form:

$$r' = \sum_{n=-\infty}^{+\infty} \sum_{m=-\infty}^{+\infty} \hat{r}_{nm}(x, y) \exp[i(\int \alpha_{nm}(\xi) d\xi + m\beta z - n\omega t)]$$

$\alpha_{nm}$  is complex,  $\beta$  and  $\omega$  are real numbers. The integers  $n$  and  $m$  characterise the frequency and the spanwise wave number, respectively. When these disturbances are introduced into the Navier-Stokes equations, a system of coupled partial differential equations is obtained; it is solved by a marching procedure, as for the linear PSE. For 2D flows, nonlinear computations end with a sudden increase of the major modes and of their harmonics; this simulates the breakdown to turbulence. For three-dimensional (3D) flows governed by a pure CF instability, the nonlinear interactions result in a saturation of the amplitude of all modes.

### 2.3. Structure of the project

In the SUPERTRAC project, the possibilities of laminar flow control on supersonic aircraft wings are investigated through 6 Workpackages (WP).

In WP1 (2005), a preparatory work has been carried out. The industrial partners provided a quantitative definition of the objectives (Mach number, Reynolds number of a supersonic aircraft), as well as the preliminary definition of a fully 3D wing which served as a reference shape.

The goal of WP2 is to investigate two important concepts:

the laminar flow control by micron-sized roughness elements (MSR), and the prevention of leading edge contamination by appropriate passive devices. Extensive computations were carried out in order to define a "large" but simple model (constant chord model) aimed at validating these concepts. Euler, boundary layer, linear and nonlinear stability computations were used to determine the most appropriate pressure gradient and the most efficient wavelength in order to validate the concept of laminar flow control by micron-sized roughness elements. In parallel, anti-contamination devices (ACD) were defined from RANS computations. The model has been manufactured and tested at supersonic Mach numbers in the S2MA wind tunnel of the ONERA Modane-Avrieux centre. Paragraph 3 describes the definition of the model and the experiments. It also presents some typical results.

The concept of laminar flow control by suction is studied in WP3. This concept was also validated by wind tunnel experiments on a simple geometry. A constant chord swept wing equipped with a suction system was defined from Euler, boundary layer and stability computations. The model was manufactured and tested in the RWG tunnel of DLR Göttingen. The work carried out within WP3 is summarized in paragraph 4.

Natural Laminar Flow (NLF) is the object of WP4. As this concept is technically simpler to apply than the concepts investigated in WP2 and WP3, it has been decided that the study will concentrate on the "numerical" model defined in WP1. Therefore this WP started at the completion of WP1 (July 2005). Here, the complexity comes from the fully 3D nature of the flow. The wing shape of WP1 was optimized (i.e. the pressure distribution was optimized) for obtaining a laminar flow extent as large as possible. An overview of the investigations of WP1 and WP4 is given in paragraph 5. The possibility of combining the optimized pressure distribution with the application of MSR, ACD and suction is currently investigated. The objective is to search the best compromise(s) between the "pure" NLF control and additional laminar flow concepts of WP2 and WP3.

In the final part of the project (end of 2007 and probably beginning of 2008), the exploitation of the results of WP2, WP3 and WP4 will be addressed in WP5. This WP is managed by the industrial partners; it will provide a summary of the results, a quantification of benefits and recommendations for the applicability of the tools investigated in the previous WP.

### 3. LAMINAR FLOW CONTROL BY MSR AND ACD (WP2)

#### 3.1. Definition of the S2MA model

Let us recall that this model will be used to validate the concept of transition control by MSR and to test devices aimed at delaying leading edge contamination. The second problem is a local one, in the sense that the absence or the appearance of leading edge contamination depends on a single parameter,  $\overline{R}^*$ , which is strongly linked to the attachment line flow. By contrast, the problem of transition control by MSR involves the pressure distribution all along the wing, from the leading edge to the transition point. Therefore both problems have been studied independently of each other and will be examined successively. In all cases, the computations have been performed in the conditions of the future experiments, i.e. for Mach numbers between 1.5 and 2, stagnation pressures from 0.50 to 1.25 bar and a total temperature of 300 K. A complete description of the model definition can be found in [10].

#### 3.1.1. Definition of the ACD

As leading edge contamination is a local problem, a simplified geometry was considered. It consists of a half-cylinder (radius = 10 mm) followed by a flat plate, see figure 1. It is fixed at a sweep angle of 65° to a solid wall representing the wind tunnel wall. It is important to keep in mind that leading edge contamination is not a *transition* problem, but a *relaminarization* problem; the goal is to model the mechanisms by which the turbulence coming from the wall can be damped (or not) by appropriate devices placed on the leading edge. For this purpose, RANS computations using several turbulence models have been performed in a computational domain comprising the simplified model and the lateral wall.

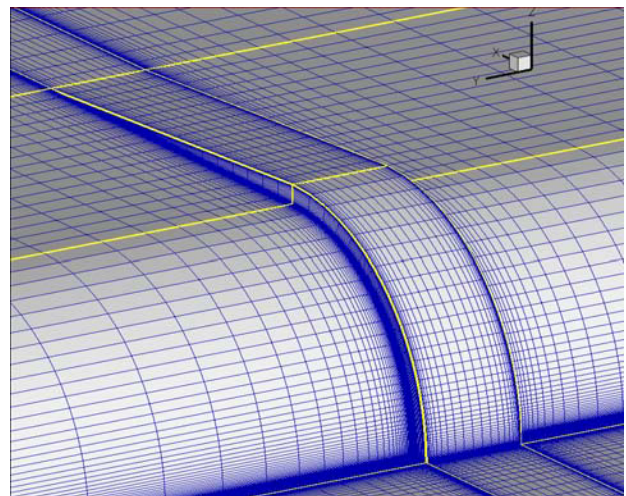


FIG. 1- Leading edge (upper half) with a "positive" ACD ("bracelet"). Grid for RANS computations

As a first step, computations were carried out for the “clean” leading edge (without ACD). As expected, the RANS computations provided the right trends (for instance the boundary layer shape factor decreased with increasing Reynolds number) but were unable to mimic the complex physics of leading edge contamination.

In a second step, ACD were installed on the leading edge. Figure 1 shows the typical shape of a “bracelet”, i.e. a “positive” device of rectangular cross section (upper half of the leading edge region) According to Creel [11], this kind of device can be efficient to relaminarize the attachment line flow at supersonic Mach numbers. Computations were also made for positive devices of triangular cross section and for “negative” devices of triangular and trapezoidal cross sections.

For the positive devices represented in figure 1, a parametric study was performed by varying the height  $h$  of the bracelets by keeping the value of  $R^*$  constant and equal to 440. The main results are:

- For small values of  $h$ , the turbulence coming from the wall “jumps” over the bracelet without any significant modification;
- For larger values of  $h$ , a stagnation point is created on the windward face of the device. However, a clear relaminarization is never observed.

The numerical results exhibited similar trends with the other shapes. The second observation above could lead to the conclusion that avoiding leading edge contamination is impossible with this kind of devices. However, as RANS models have shown their inability to model leading edge contamination on a clean leading edge, this conclusion could be too pessimistic. Therefore it was decided that the appearance of a stagnation point would be the criterion for an efficient ACD.

### 3.1.2. Definition of the MSR

The numerical work was undertaken for two different (theoretical) wing profiles, one proposed by ONERA, the other proposed by Dassault-Aviation. The first one is a symmetrical airfoil profile at zero angle of attack, with a blunt nose and a circular main body; its relative thickness is 20%. The second profile is not symmetrical and much thinner (around 6%), with a very small leading edge radius; the computations were done for an angle of attack of  $3.5^\circ$ . In both cases, the chord normal to the leading edge was fixed to 0.4 m. The free-stream Mach number, the sweep angle and the unit Reynolds number were varied systematically in the calculations, which were shared between the partners involved in this Task.

The theoretical  $C_p$  distributions are plotted in figure 3 for the two airfoils at a sweep angle of  $30^\circ$ . The flow acceleration around the leading edge is stronger for the Dassault airfoil, and rather weak further downstream.

Then a linear stability analysis and the  $e^N$  method gave an estimated point of transition as well as an indication of modes that are most likely to cause transition. On the basis of these computations, a few cases were selected that had an estimated transition point in the first half of the chord.

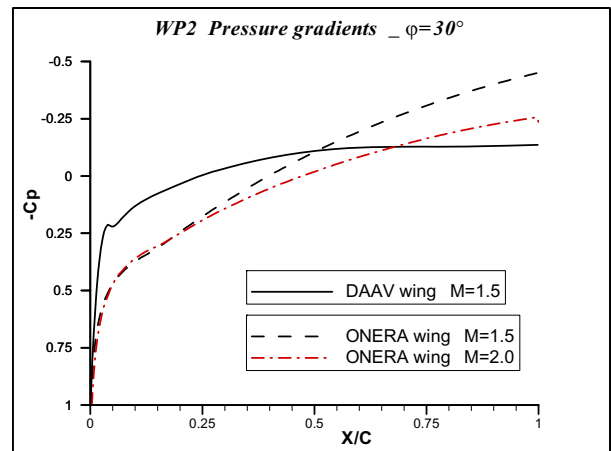


FIG. 2-  $C_p$  evolution for the Dassault (DAAV) and ONERA airfoil profiles, sweep angle =  $30^\circ$

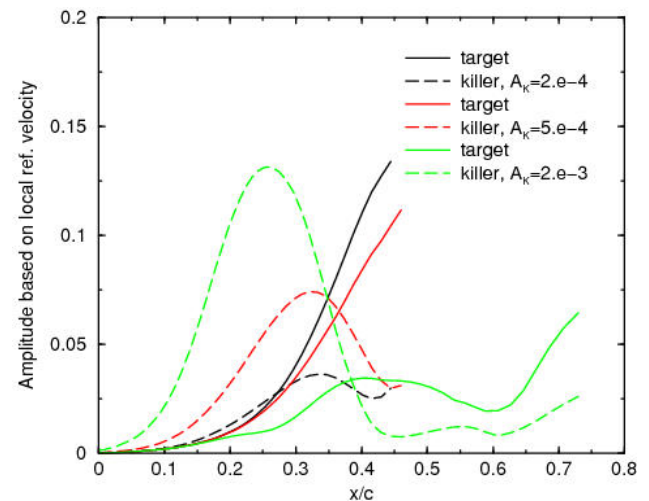


FIG. 3- Nonlinear PSE computations for the ONERA airfoil profile

Non linear stability analyses were carried out on the selected cases. Many interaction scenarios were investigated by systematic variations of the killer mode initial amplitude and wavelength. Figure 3 presents examples of “interesting” results for the ONERA airfoil at Mach 1.5. The stagnation pressure is 0.75 bar and the sweep angle  $20^\circ$ . The target mode corresponds to  $\beta = 3000 \text{ m}^{-1}$ , i.e.  $\lambda = 2\pi/\beta = 2.1 \text{ mm}$ . Its initial amplitude  $A_t$  is equal to  $5 \cdot 10^{-4} u_e$ , where  $u_e$  is the local free-stream velocity. The killer mode corresponds to  $\beta = 4500 \text{ m}^{-1}$ , i.e.  $\lambda = 1.4 \text{ mm}$ . The figure shows the evolution of the amplitude of the killer modes (dotted lines) and of the target modes (full lines) for three values of the initial amplitude  $A_k$  of the killer mode. Different values of  $A_k$

correspond to different roughness heights. Numerically, the target is the (0,2) mode, the killer is the (0,3) mode, the (0,1) mode corresponding to  $\beta = 1500 \text{ m}^{-1}$ . This mode and other modes up to (0,9) have been taken into account in the computations but are not plotted for the sake of clarity. Increasing  $A_k$  clearly reduces the growth of the target mode but at the same time accelerates the growth of the killer mode (and of the other modes), so that it is difficult to estimate how the combination of these phenomena will affect the point of transition. One can imagine that there exists an optimum value of  $A_k$  for which transition is delayed. The link between  $A_k$  and the roughness height was estimated from receptivity computations performed by DLR.

### 3.1.3. Manufacturing of the model

After the non linear computations have been completed, a comparison between the performances of the ONERA and Dassault airfoils led to the conclusion that the most promising interaction scenarios were found for the ONERA airfoil. The explanation is the following. As shown in figure 2, the Dassault airfoil exhibits a weak negative pressure gradient beyond 25% chord. This implies that transition is not completely governed by CF instability in this region, so that the control by roughness elements (which is based on the properties of the CF waves) becomes more difficult. Technological arguments are also in favor of the ONERA airfoil. Due to the small relative thickness of the Dassault airfoil, sticking the roughness elements on its thin leading edge could be very difficult; in addition, risks of flutter and bending during the wind tunnel runs could not be neglected.

The wing was manufactured by ONERA. As mentioned before, the chord normal to the leading edge was 0.4 m. The span was around 1.5 m. The model was made of two parts, a removable leading edge and the main body. It was equipped with two rows of pressure taps. Large areas on the body were covered with insulating material (white part of the wing in Figure 4) in order to make possible infra red (IR) measurements for the MSR experiments. The approximate thickness of the insulating layer was 1 mm. Transition was detected by 4 IR cameras, 2 for the upper side (inboard and outboard), 2 for the lower side (inboard and outboard). As IR thermography is not suitable for studying leading edge contamination, the efficiency of the ACD was checked by looking at the signals delivered by three hot films flush mounted close to the attachment line, one upstream of the ACD position (in the spanwise direction), two downstream of this position.

The MSR were small cylinders normal to the wall. Due to the uncertainty in the theoretical definition of the “best” roughness elements, 5 rows of about 30 elements each were installed on the model leading edge, at a distance of 5 to 8 mm from the attachment line. For each row, the spanwise wavelength of the MSR was constant, with values from 1.4 to 2.1 mm. The diameter of the elements

was 0.15 mm for one row, 0.20 mm for the other four rows. Their height was 10  $\mu\text{m}$  in all cases. Two rows were installed on the lower side (one inboard, one outboard), three on the upper side (2 inboard, one outboard). The 4 IR cameras made it possible to determine **simultaneously** the boundary layer state (laminar or turbulent) downstream of the rows. The spanwise distance between two rows was large enough to observe the location of the “natural” transition.

Seven ACD shapes were selected and manufactured by ONERA with a small part of the model leading edge. They were inserted **successively** on the leading edge at a distance of about 45 cm from the wind tunnel wall, i.e. far enough from the turbulent boundary layer developing on this wall.

## 3.2. Experiments

The test campaign in the S2MA wind tunnel took place in October 2006. The experiments were carried out at zero angle of attack. Figure 4 shows a photograph of the model installed in the test section.



FIG. 4- Swept wing model in the S2MA wind tunnel.

The MSR were tested at sweep angles  $\phi$  from 15 to 30°, for several stagnation pressures between 0.5 and 1.25 bar and for two Mach numbers, 1.5 and 2. In the chosen sweep angle range, the estimated  $\overline{R}$  Reynolds number was lower than the critical value 250. As a consequence, the MSR experiments were expected to be free of any risk of leading edge contamination. For the ACD tests, the sweep angle was fixed to  $\phi = 65^\circ$ , for which leading edge contamination occurred. Two Mach numbers (1.7 and 2.7) and several stagnation pressures (from 0.3 to 1.4 bar) were considered for these experiments.

### 3.3. Analysis of the results

Although the analysis of the results has not been completed yet, some important features have already been identified. The detailed results will be published in the near future in dedicated papers.

Comparisons were made between the measured and theoretical  $C_p$  distributions assuming the infinite swept wing assumption. The agreement is excellent when the leading edge is supersonic, i.e. for all the MSR experiments and for the ACD experiments at Mach 2.7. In the case of a subsonic leading edge (ACD experiments at Mach 1.7), strong differences appear. For this “pathological” case, fully 3D Euler computations performed by IST substantially improved the agreement, which demonstrates that the discrepancies are mainly due to 3D effects and not to viscous effects.

As far as  $\overline{R^*}$  is concerned, the “exact” values deduced from the measured pressure gradient around the leading edge are substantially larger than those given by the compressible counterpart of the simple cylinder formula given in paragraph 2.1.2. The difference is around 30% for the MSR experiments (low  $\phi$ ), it reaches 40% for the ACD experiments (large  $\phi$ ).

The analysis of the ACD efficiency was based on the evolution of the hot film rms levels as a function of the total pressure  $Pt$ . It turned out that for both Mach numbers (1.7 and 2.7), leading edge contamination starts at  $\overline{R^*} \approx 270$ , in good agreement with the criterion [6]. One of the ACD delays contamination up to  $\overline{R^*} \approx 320$  for  $M = 1.7$ , up to  $\overline{R^*} \approx 400$  for  $M = 2.7$ , whilst the other devices do not show any significant improvement by comparison with the “clean” leading edge case.

From the infra red images, the transition location was detected downstream of the MSR as well as in the intervals between the MSR rows. In the latter cases, which correspond to the “natural” transition, the measurements are correlated with  $N$  factors between 8.5 and 11. These  $N$  factors were computed for the stationary vortices using the nonlocal fixed  $\beta$  strategy. Downstream of the MSR no positive effect is observed: in all cases, transition takes place a short distance upstream of its “natural” position. However transition is never tripped immediately downstream of the roughness elements. Possible explanations to the lack of efficiency are the too large size of the elements (height, diameter), as confirmed by receptivity computations carried out by DLR, and the too small number of elements in each row (disturbances are generated by the two extreme elements).

## 4. LAMINAR FLOW CONTROL BY SUCTION (WP3)

As explained in paragraph 2.3, this part of the SUPERTRAC project is aiming at the extension of the technology of laminar flow control by suction to aircraft operating at supersonic speeds. More precisely, it was planned to investigate the suction effects on pure CF transition. As for the S2MA model, the first year of the project was devoted to the numerical definition of the swept wing model to be tested in the RWG wind tunnel at DLR Göttingen. Again a model with constant chord was considered for the sake of experimental and numerical simplicity.

The characteristics of the wind tunnel imposed the following constraints: Mach number  $M = 2$ , chord normal to the leading edge  $c = 0.3$  m, stagnation temperature = 244 K, stagnation pressure from 1.2 to 3.6 bar, sweep angle  $\phi = 20$  to  $30^\circ$ .

### 4.1. Definition of the RWG model

#### 4.1.1. Choice of the airfoil profile

At the beginning, it was decided to use a symmetrical airfoil at zero angle of attack, but the relative thickness of the model had to be specified. A preliminary definition phase showed that a 13% relative thickness was necessary to observe a significant crossflow instability. In addition it was not obvious whether a sharp or blunt leading edge would better meet the demands. The corresponding profile contours for the two candidates are shown in figure 5.

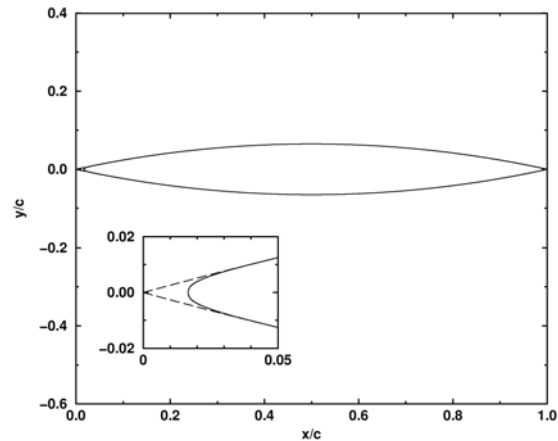


FIG. 5- Sharp and blunt profile contours

Systematic computations were carried out to assess the advantages and drawbacks of the two solutions. The technological difficulties for the implementation of the suction panel were also taken into account. The analysis showed that a sharp leading edge was probably superior. Thus, only the sharp leading edge model was considered in the subsequent analysis for the identification of the optimal position and extent of the suction panel. In the computations, the sweep angle  $\phi$  was fixed to  $30^\circ$ .

#### 4.1.2. Definition of the suction panel

A large amount of computations was shared between the partners in order to investigate systematically the effect of the following parameters: starting point and streamwise extent of the suction panel; stagnation pressure; suction mean velocity  $V_w$ , with values from 0 to  $-0.46 \text{ ms}^{-1}$  (it was assumed that  $V_w$  was constant in the sucked region).

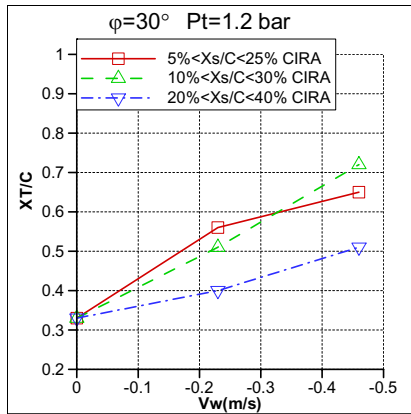


FIG. 6- Effects of the suction velocity and length on the transition location

Linear stability computations were carried out and transition was assumed to occur for a critical  $N$  factor equal to 8. As an example of result, figure 7 presents the theoretical variation of the transition location as a function of the suction velocity  $V_w$ , for  $\varphi = 30^\circ$  and a stagnation pressure equal to 1.2 bar. Suction starts at 5, 10 or 20% chord, and is applied along a constant streamwise distance of 20% chord. Its effect on transition is very strong. As found previously in subsonic and transonic applications, this effect is more pronounced when suction begins close to the point where the unstable waves start to be amplified (between 5 and 10% chord in the present case).

The previous results were obtained assuming a constant value of  $V_w$  along the suction panel length. Additional computations were performed in order to optimize the streamwise mass flow distribution  $m_w = \rho_w V_w$  ( $\rho_w$  is the density at the wall). The total mass flow rate was imposed, as well as the position and length of the suction panel. The goal was to minimise the disturbance kinetic energy in a given control domain. The numerical results showed that using the optimal suction distribution resulted in significantly lower  $N$  factors by comparison with the constant suction velocity case.

#### 4.1.3. Final design of the model

During the final design of the suction system, it was decided that the suction panel will extend from 5 to 20% chord. Moreover, assuming a constant pressure in the suction chamber and using an empirical law for the pressure drop across the perforated wall led to the

conclusion that the resulting suction velocity distribution was close to the optimal suction distribution. Therefore a single suction chamber seemed to be sufficient to meet the objectives. A sketch of the suction model is shown in figure 7.

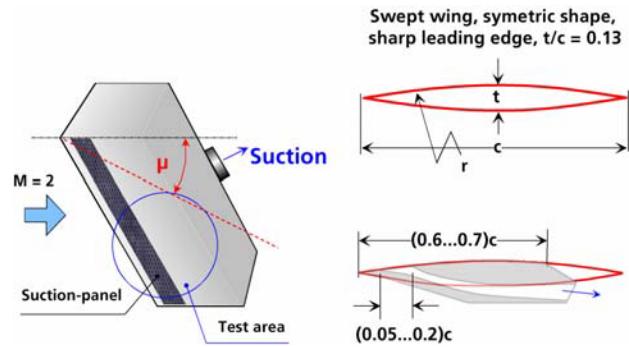


FIG.7- Sketch of the suction model

The suction panel was manufactured from a permeable sinter filter element that was carefully polished before it was contoured and mounted on the model. The suction characteristics of the sinter sheet were calibrated after the mounting in the breadboard constructions at various pressure differences and levels. The thickness of the sheet was 3 mm. The equivalent hole-diameter was  $17 \mu\text{m}$  and the volume porosity 43%. Transition was detected by optical methods, quantitative infrared thermography (QIRT) and global skin friction interferometry (GISF), often named also oil-film interferometry. The pressure distribution on the model surface was measured by four pressure taps.

#### 4.2. Experiments

The measurements were performed in the DLR Göttingen Ludwig Tube Facility (DNW-RWG) at Mach 2. Three test cases have been investigated:

- two cases with a sweep angle  $\varphi = 30^\circ$  and two stagnation pressures,  $Pt = 1.2$  (case 1) and 1.8 bar (case 2), corresponding to unit Reynolds numbers close to  $17 \cdot 10^6 \text{ m}^{-1}$  and  $25 \cdot 10^6 \text{ m}^{-1}$ , the stagnation temperature being around 275 K;
- one case with  $\varphi = 20^\circ$  and  $Pt = 2.3$  bar (case 3), corresponding to a unit Reynolds number close to  $30 \cdot 10^6 \text{ m}^{-1}$  with a stagnation temperature around 290 K.

The suction velocity was varied as a free parameter between 0 and approximately  $1 \text{ ms}^{-1}$ .

#### 4.3. Analysis of the results

Significant differences between numerical and measured pressure distributions were observed for  $\varphi = 30^\circ$ . They could be explained by the reflection of the leading edge shock wave on the wind tunnel wall.

Without suction, the transition  $N$  factors for stationary and travelling waves are around 6 for  $\varphi = 30^\circ$  and around

8.5 for  $\varphi = 20^\circ$  (according to linear PSE computations). A slight increase in  $N$  is detected for increasing unit Reynolds number. This seems to indicate that travelling CF waves play a more important role in these experiments than in the S2MA experiments.

The variation of the transition Reynolds number as a function of the suction velocity is plotted in figure 8 for the three cases. Suction leads to the expected delay of transition. This effect is more pronounced for  $\varphi = 30^\circ$  than for  $\varphi = 20^\circ$ . In all cases, the transition location seems to reach an “asymptotic” position when the suction rate increases. This asymptote is reached more rapidly for  $\varphi = 20^\circ$  than for  $\varphi = 30^\circ$ . From a practical point of view, it is important to know if a constant value of the transition  $N$  factor (for a given configuration) is able to correlate the experimental data without and with suction. Computations are in progress in order to answer this question.

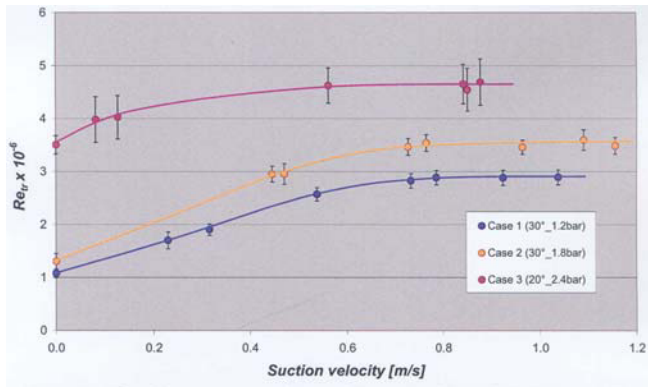


FIG. 8- Effect of suction on the transition Reynolds number (fixed unit Reynolds number for each curve)

## 5. LAMINAR FLOW CONTROL BY SHAPE OPTIMISATION (WP1 AND WP4)

The starting point of this part of the project is a realistic fully 3D wing in flight conditions. This wing was selected by the industrial partners in WP1. It was then used in WP4 with two objectives: firstly, to assess precisely the natural laminar flow extension and secondly to propose geometry modifications in order to improve it, accounting for different constraints (e.g. geometrical and specified value of lift). Finally, the compatibility between the optimized wing and the laminar flow control techniques of WP2 and WP3 is analyzed.

### 5.1. Baseline configuration

During the first months of the project, the two industrial partners (Airbus-UK and Dassault Aviation) reviewed options for a baseline supersonic commercial aircraft configuration. After several iterations, the following flow

conditions have been chosen:

- Mach number = 1.6
- Altitude = 44 000 ft
- Semi span = 9.35 m
- Reference chord  $C_{ref} = 7$  m, corresponding to a chord Reynolds number =  $58 \cdot 10^6$ .

The wing characteristics (planform, thickness, twist and camber) have also been defined. The lift coefficient  $C_L$  is 0.18, corresponding to an angle of attack close to  $4^\circ$ . The wing planform is shown in figure 9.

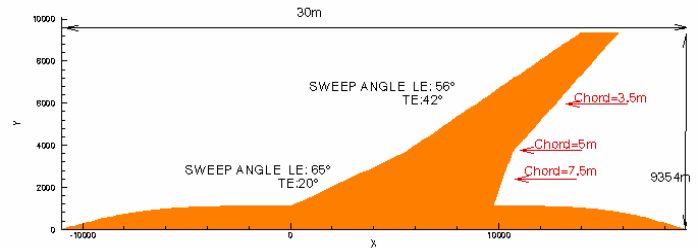


FIG. 9 – Planform of the baseline configuration  
LE: leading edge, TE: trailing edge

### 5.2. Shape optimization

Euler, boundary layer and linear stability computations rapidly demonstrated that the proposed baseline wing was fully turbulent. A parametric study of some parameters (angle of attack, sweep angle, relative thickness) did not improve significantly the results.

As a consequence, it was decided to start again with a completely new wing shape. As a first step, a preliminary optimization was done with a constant geometry representative of a mid-span wing section of the fully 3D airfoil described before. This work was performed by CIRA using a genetic algorithm, according to the design conditions and to the requirements given by Dassault Aviation. From this simple wing, Dassault designed a fully 3D airfoil which was used as the new baseline geometry for the optimization process.

ONERA and CIRA were in charge of this optimization, which consisted in maximizing the laminar extent of the outboard upper part while maintaining the performance (lift and pitching moment constraints) in non-viscous assumptions. The numerical tool used by CIRA is based on a multi-objective genetic algorithm with the Pareto dominance criterion. ONERA also employed a software based on a genetic algorithm and took into account the presence of the fuselage. For transition prediction, both partners used the simplified  $e^N$  method (data base method) developed by ONERA [12].

The results of these computations were two optimized wings, one designed by CIRA, the other by ONERA. In both cases, the transition process is dominated by TS and traveling CF waves. The stationary CF vortices seem to play a minor role. The laminar flow extension varies

along the spanwise direction from a few percent chord to about 20% chord. A detailed analysis of the results is in progress in order to decide which airfoil will be kept for further investigations.

### 5.2.1. Compatibility of the different control techniques

The current work in this WP consists in a numerical investigation of the compatibility between the pressure field of the two optimized wings and the laminar flow control techniques studied in WP2 and WP3. Although the work is not yet completed, some trends have already been identified:

i) In design conditions, the  $\overline{R^*}$  Reynolds number along the attachment line remains below the critical value 250. However, leading edge contamination is likely to occur in off-design conditions, so that some ACD will be necessary. Let us recall that an efficient ACD was tested during the S2MA experiments.

ii) The pressure gradients resulting from the Natural Laminar Flow optimizations are not suitable for a control by MSR.

iii) Suction is much more efficient for delaying transition when applied on the optimized pressure distributions than on the baseline pressure field.

## 6. CONCLUSION

The work performed within SUPERTRAC focused on three models: two physical models (constant chord swept wings) tested in appropriate wind tunnels and a "numerical" (and more realistic) model.

The first model was designed and tested in the S2MA facility in order to investigate the efficiency of anti-contamination devices (ACD) and of micron-sized roughness elements (MSR). The second model was used for studying the wall suction effects on laminar-turbulent transition in the RWG wind tunnel. Beside classical techniques based on the local, linear stability theory, advanced numerical tools were employed in the design phase of the models: non linear PSE for MSR, 3D RANS computations for ACD, optimization procedures for suction. From a practical point of view, positive results were obtained for ACD and for suction, while the MSR experiments proved to be much more difficult to conduct, at least from a technological point of view. The last months of the project will be devoted to complete the analysis of the experimental data.

The numerical model, selected by the industrial partners, was a fully 3D wing in flight conditions. As a first step, advanced optimization procedures (genetic algorithms) were used in order to increase the natural laminar flow (NLF) area as much as possible. As a second step, a compatibility analysis between NLF, MSR, ACD and suction has been undertaken. This will lead to the definition of the "best" supersonic wing combining

different laminar flow control devices in the best way. The last part of SUPERTRAC will be devoted to a quantification of benefits and recommendations for the different tools investigated previously.

It is hoped that the fundamental, numerical and experimental investigations carried out during the project will result in firm conclusions regarding the possibilities of designing a supersonic airfoil with extended laminar flow.

### Acknowledgement

The investigations presented in this paper have been obtained within the European research project SUPERTRAC under contract No AST4-CT-2005-516100. The author is grateful to the SUPERTRAC partners for providing the results discussed in the paper.

### References

- [1] W.S. Saric, R.C. Carrillo, M.S. Reibert: Leading edge roughness as a transition control mechanism, AIAA Paper 98-0781, 1998
- [2] W.S. Saric, H.L. Reed: Supersonic laminar flow control on swept wings using distributed roughness, AIAA Paper 2002-0147, 2002
- [3] W.S. Saric, H.L. Reed: Crossflow instabilities. Theory and technology, AIAA Paper 2003-0771, 2003
- [4] W. Pfenninger: Flow phenomena at the leading edge of swept wings, AGARDograph 97, Part 4, 1965
- [5] D.I.A. Poll: Some aspects of the flow near a swept attachment line with particular reference to boundary layer transition, Technical Report 7805/K, Cranfield, College of Aeronautics, 1978
- [6] D.I.A. Poll: Boundary layer transition on the windward face of space shuttle during reentry, AIAA Paper 85-0899, 1985
- [7] J. Reneaux, J. Preist, D. Arnal, J.C. Juillen: Control of attachment line contamination, 2<sup>nd</sup> European Forum on Laminar Flow Technology, Bordeaux, June 1996
- [8] T. Herbert: Parabolized Stability Equations, AGARD Report 793, 1993
- [9] D. Arnal: Boundary layer transition prediction based on linear theory, AGARD Report 793, 1993
- [10] D. Arnal, C.G. Unckel, J. Krier, J.M. Sousa, S. Hein: Supersonic laminar flow control studies in the SUPERTRAC project, 25th ICAS congress, Hamburg, 3-8 September 2006
- [11] T.R. Creel: Effects of sweep angle and passive relaminarisation devices on a supersonic swept-cylinder boundary layer, AIAA Paper 91-0066, 1991
- [12] G. Casalis, D. Arnal: ELFIN II, Subtask 2.3: Data base method. Development and validation of the simplified method for pure crossflow instability at low speed, CERT/ONERA Report 119/5618.16, December 1996